

Shell Cross-Linked Hyaluronic Acid/Polylysine Layer-by-Layer Polyelectrolyte Microcapsules Prepared by Removal of Reducible Hyaluronic Acid Microgel Cores

Hyukjin Lee, Yongho Jeong, and Tae Gwan Park*

Department of Biological Sciences, Korea Advanced Institute of Science and Technology,
Daejeon 305-701, South Korea

Received April 1, 2007; Revised Manuscript Received September 19, 2007

Shell cross-linked hollow polyelectrolyte microcapsules composed of hyaluronic acid (HA) and poly-L-lysine (PLL) were prepared by layer-by-layer (LBL) adsorption and subsequent core removal by a reductive agent. Disulfide cross-linked HA microgels were used as template core materials for the LBL deposition on the surface and removed by treatment of dithiothreitol at neutral pH condition. HA/PLL polyelectrolyte multilayers on the shell were chemically cross-linked via carbodiimide chemistry, and their physicochemical properties and drug release behaviors were investigated. Shell cross-linked HA/PLL polyelectrolyte microcapsules exhibited far enhanced physical stability against freeze–thaw cycles and acidic pH conditions compared to the un-cross-linked ones. The cross-linked HA/PLL multilayer shell also demonstrated pH responsive permeability, which became more permeable at low pH than at neutral pH. When bovine serum albumin (BSA), as a model protein drug, was loaded inside using the pH-dependent permeability, BSA release profiles from the microcapsules could be readily modulated by varying medium pH values or adding an HA digesting enzyme (hyaluronidase) in the incubation medium.

Introduction

Polymeric microcapsules composed of polyelectrolyte multilayers have drawn much interest during the past few years due to their versatile uses in drug delivery systems and microreactors for synthesis of inorganic particles.^{1–6} Development of a layer-by-layer (LBL) self-assembly technique allows an easy and cost-effective method for preparing polyelectrolyte multilayer capsules. Electrostatic interactions between oppositely charged polyelectrolytes enable alternating adsorptions of charged polymer species onto the surface of core materials. Hollow multilayered polyelectrolyte microcapsules can be readily obtained after removing the core materials. The physicochemical properties of these LBL microcapsules are well-characterized in many previous studies.^{7–9}

Among these microcapsules, environmentally responsive polyelectrolyte microcapsules can serve as ideal materials for drug delivery applications, since smart drug delivery systems often require a countertalk with an external stimulus.^{10,11} Depending on the selection of layer materials, hollow microcapsules could exhibit distinct and reversible changes in physical properties such as size, shape, and permeability in response to external stimuli such as pH, salt, light, and metabolites.^{9,12–14} Particularly, multilayered microcapsules exhibiting a pH-responsive permeability change are of interest for many drug delivery applications.^{15,16}

However, the LBL microcapsules primarily fabricated from relatively weak electrostatic interactions between cationic and anionic polymers often exhibit inherent structural instability and lack of biocompatibility, limiting their practical applicability. It is essential to prepare robust microcapsules that show resilient properties against various environmental stresses such as pH, ionic strength, and freeze/thawing. One of the promising

methods to improve the stability of polyelectrolyte LBL microcapsules is to covalently cross-link LBL multilayered walls.^{17–19} For instance, LBL microcapsules composed of poly(acrylic acid) (PAA) and poly(allylamine hydrochloride) (PAH) were shell cross-linked before core removal by EDC to improve capsule stability.¹⁸ Photosensitive diazoresin was incorporated in the LBL multilayer that was cross-linked later by UV radiation to confer better stability against solvent etching and osmotic pressure.¹⁹ Biocompatibility of polyelectrolyte materials is also a major concern when they are used as drug carriers. Naturally occurring anionic polysaccharides such as hyaluronic acid (HA) and alginate in combination with cationic peptides and polysaccharides were used to fabricate more biocompatible LBL multilayers.^{20–22} In fact, HA is a major constituent of extracellular matrix composed of *N*-acetyl-D-glucosamine and D-glucuronic acid and exhibits excellent biocompatibility and biodegradability which can be widely used for many drug delivery applications.²³

Previously we reported HA spherical nanogels for delivery of siRNAs by self-cross-linking of thiolated HA using an inverse emulsion method.²⁴ In this study, disulfide cross-linked HA microgels were fabricated by an inverse suspension method, onto which HA and poly-L-lysine were alternatively adsorbed to form an LBL multilayer shell. The HA microgel cores were then removed by using a reducing agent, followed by chemical cross-linking of HA/PLL multilayers. It was expected that reducible HA microgels, compared to the conventional organic and inorganic core materials, not only could serve for anionic temporal templates for LBL multilayer growth but also offer the opportunity for encapsulation of various macromolecular drugs.^{24,25} The cross-linked hollow HA/PLL microcapsules were characterized in terms of structural stability against pH alteration and freeze/thawing. Fluorescein isothiocyanate (FITC)-labeled bovine serum albumin (BSA) was used as a model protein drug to encapsulate within the microcapsules by utilizing pH-

* Corresponding author: tel, +82-42-869-2621; fax, +82-42-869-2610; e-mail address, tgpark@kaist.ac.kr (T. G. Park).

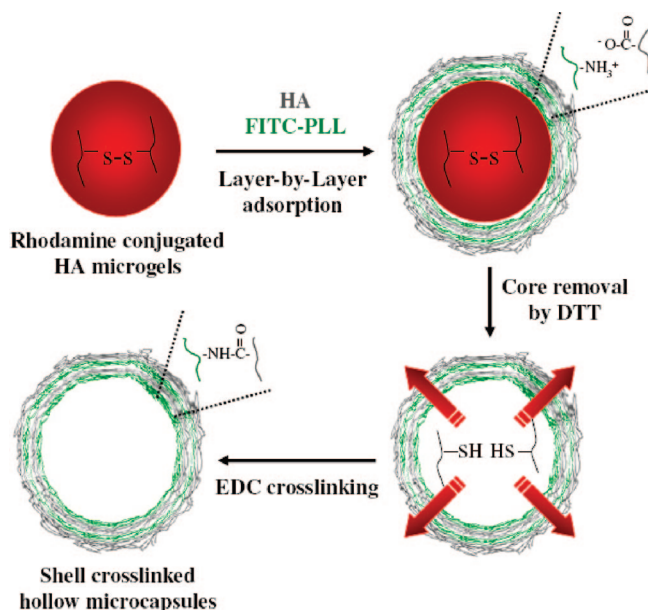


Figure 1. Schematic illustration for fabrication of cross-linked hollow LBL HA/PLL microcapsules.

dependent change of permeability in the cross-linked LBL wall. FITC-BSA release patterns from the HA/PLL microcapsules were also examined by analyzing a fluorescence increase in the incubating medium at different pH values and in the presence of an HA digesting enzyme, hyaluronidase.

Experimental Section

Materials. Hyaluronic acid (HA) sodium salt (MW 17 and 64 kDa) was purchased from Lifecore Biomedical (Chaska, MN). Poly-L-lysine hydrobromide (PLL) (MW 39 kDa), FITC-dextran (150 kDa), FITC-BSA (66 kDa), [1-ethyl-3-(dimethylamino)propyl]carbodiimide hydrochloride (EDC), hyaluronidase, dithiothreitol (DTT), and cystamine were all obtained from Sigma-Aldrich (St. Louis, MO). Cell counting kit-8 (CCK-8) was obtained from Dojindo Laboratories (Kumamoto, Japan). All chemicals were used as received. Water used in all experiments was prepared by Millipore Milli-Q Plus system with a resistivity higher than 18.2 MΩ cm. Rhodamine conjugated HA was prepared by conjugating amino-rhodamine to the carboxylic groups of HA as reported previously.²⁴ FITC was conjugated to PLL as described elsewhere.²⁶

Preparation of Shell Cross-Linked Microcapsules. A schematic illustration for preparation of hollow HA/PLL LBL microcapsules is shown in Figure 1. Thiolated HA (MW 17 kDa) was prepared by reacting HA (500 mg) with an excess amount of cystamine (844 mg) in the presence of EDC (716 mg) in 50 mL of PBS (pH 7.4) solution. Cystamine having two primary amines linked by a disulfide linkage was conjugated to carboxylic acid groups in HA. The cystamine conjugated HA was treated with DTT (693 mg) for 12 h in 50 mL of PBS (pH 7.4) solution to cleave the disulfide linkage, dialyzed extensively against deionized water for 2 days, and freeze-dried. HA was then analyzed by Ellman's assay to determine the degree of thiol incorporation, and estimated thiol modification ranged from 30 to 40%.²⁴ Thiolated HA was dissolved in 4 mL of PBS (pH 8.0) solution at a concentration of 10 % (w/v). The aqueous solution was slowly added to 100 mL of hexane under vigorous stirring condition at 2000 rpm to generate a water-in-oil inverse suspension solution. To initiate oxidative self-cross-linking of thiolated HA via the formation of disulfide bonds, 200 μL of 5 % (v/v) H₂O₂ was added to the hexane phase and the mixture was stirred for 3 h. Cross-linked HA microgels were collected by centrifugation and washed three times with a mixture of water/acetone (80:20 (v/v)). For the LBL polyelectrolyte deposition,

aqueous HA (MW 64 kDa, 5 mg/mL) and PLL-FITC (2 mg/mL) solutions containing 0.15 M NaCl were prepared at pH 6.5 by adding 0.1 M NaOH or 0.1 M HCl. Alternative LBL adsorption of HA and PLL onto the surface was conducted by incubating the HA microgels in each polyelectrolyte solution for 10 min followed by centrifugation at 1000 rpm and three washing steps with 0.15 M NaCl solution. After the desired number of HA/PLL layers was deposited, LBL-coated HA microgels were collected by centrifugation at 1000 rpm and incubated in 100 mM DTT solution for 12 h at pH 7.0 with continuous shaking to remove core HA microgels. The hollow microcapsules were washed with 0.15 M NaCl solution for several times to remove residual HA, and incubated in 5 % (w/v) EDC solution for 6 h to obtain shell cross-linked microcapsules. The resultant microcapsules were collected by centrifugation at 2000 rpm for 5 min, washed gently, and resuspended in water for further analysis.

ζ-Potential Measurement. HA/PLL multilayer growth on the surface of HA microgels was analyzed by measuring the ζ-potential value of the LBL-coated microgels using a zeta potential measuring instrument (Zeta-Plus, Brookhaven, NY). After each adsorption step, LBL microgels were resuspended in 3 mL of deionized water and the surface ζ-potential value was recorded ($n = 5$). All measurements were performed at pH 6.5.

Confocal Laser Scanning Microscopy (CLSM). Confocal images of HA microgels and HA/PLL LBL polyelectrolyte microcapsules were obtained using a confocal laser scanning microscope (LSM 510, Carl-Zeiss Inc., USA) at an excitation wavelength of 488 nm for green fluorescence and at an excitation wavelength of 543 nm for red fluorescence, respectively. Cross-linked HA microgel cores were visualized by using rhodamine-labeled HA (17 kDa), while LBL polyelectrolyte multilayers formed on the surface were observed by using FITC-labeled PLL. The structural integrity of the microcapsules with and without shell cross-linking was examined under a confocal microscope. Both cross-linked and un-cross-linked microcapsules were treated with three cycles of freezing/thawing for verifying the enhanced mechanical and thermal stability of cross-linked capsule walls, while the capsule stability upon pH changes were also tested under a confocal microscope as a function of incubation time in acidic pH condition (pH 2.0). For determination of pH-dependent permeability, shell cross-linked polyelectrolyte capsules were incubated with 2 mg/mL of FITC-dextran (MW 150 kDa) for 15 min at two different pH conditions. The images were taken under acidic (pH 2.0) and neutral (pH 7.0) conditions.

BSA Release from Hollow HA/PLL Microcapsules. To determine pH-dependent and enzyme-mediated sustained release patterns of FITC-BSA (MW 66 kDa), HA/PLL microcapsules were incubated with FITC-BSA (2 mg/mL) solution at pH 5.0 for 2 h. After FITC-BSA was encapsulated, the microcapsules were washed gently with PBS (pH 7.0) solution and re-collected by centrifugation at 2000 rpm for 3 min. Collected microcapsules were resuspended with 10 mL of PBS (pH 7.0) solution, then 200 μL of the microcapsule suspension was distributed into the Transwell (6.5 mm diameter, 0.4 μm pore size, polycarbonate membrane, Corning Inc., Corning, NY). Each Transwell was placed in 24-well plates with 1 mL of buffer solution added in each well. Cumulative BSA release at two different pH conditions was evaluated at varied time points using a fluorophotometer. After the microcapsules were incubated at desired time periods, the Transwell was removed from the 24-well plates and the supernatant was collected for fluorescence measurement. The standard curve was generated using a stock of solution of 2 mg/mL of FITC-BSA and three repeated experiments were performed to generate mean and standard deviations of cumulative BSA release from the microcapsules. The enzyme-dependent release of BSA from the microcapsules was similarly obtained except for adding different amounts of hyaluronidase (10 or 50 U/mL) in buffer solution at pH 7.0.

Cytotoxicity Test. To evaluate cytotoxicity of HA/PLL microcapsules, NIH3T3 and C2C12 cells were used. The cells were cultured in DMEM supplemented with 10% fetal bovine serum and plated in CDV

96-well flat-bottomed plate with a density of 5000 cells per well. After 24 h incubation, 50 μ L of microcapsules suspension with various concentrations was added into each well. After the microcapsules were incubated for 3 days, a number of viable cells were counted using the CCK-8 cell viability assay kit.²⁶

Results and Discussion

Preparation of Shell Cross-Linked Hollow Microcapsules. Thiol-conjugated HA (MW 17k Da) was used to fabricate core templates for the LBL adsorption. Oxidative self-cross-linking between the HA chains readily occurred via the formation of disulfide linkages within the aqueous droplets dispersed in the continuous hexane phase. The resulting HA microgel beads had an average diameter of $16.2 \pm 8.3 \mu\text{m}$ ($n = 30$) and the self-cross-linked microgels were easily disintegrated by addition of DTT (100 mM) within a few hours at neutral pH condition. The reducible hydrogel cores as LBL template materials have several distinctive advantages over conventional organic and inorganic core materials such as polystyrene, melamine formaldehyde (MF), and MnCO_3 particles. The reducible HA microgels, after the LBL deposition on the surface, can be easily removed under mild reductive aqueous conditions. For the organic and inorganic particles, more harsh processing conditions were employed to completely dissolve out the core materials. For example, polystyrene cores were often removed by an exposure to organic solvents, and inorganic cores were removed under highly acidic conditions such as 0.1 M HCl.^{7–9,27} During the harsh core removal process, LBL capsule wall properties including permeability were drastically changed due to their instability in extreme conditions.^{9,28} In conjunction with the mild core removal condition, reducible hydrogel cores offer another merit for the encapsulation of bioactive molecules before the LBL adsorption. Bioactive macromolecular drugs such as proteins, peptides, and genes can be co-dissolved in the thiolated HA solution and encapsulated into the hollow LBL microcapsules after the core removal.²⁴ Hollow LBL microcapsules containing the drug molecules inside can be also utilized as a reservoir-type controlled-release system.²⁹ This type of drug release system can offer sustained release of various drugs in a prolonged period.

Previously, various cross-linked hydrogel cores, such as Ca–alginate and dextran–HEMA hydrogels were used to grow LBL polyelectrolyte multilayers on the surface to modulate drug release rates from the core.^{22,30} The core hydrogel beads were removed by using calcium chelating agents or chemical degradation under acidic conditions to fabricate hollow LBL microcapsules. Alternatively LBL multilayer coated alginate hydrogel beads were used without removing the core as a monolithic matrix-type delivery system.³¹ Those systems could attain more sustained drug release profiles by coating a LBL multilayer on the surface, which functioned as an additional diffusion barrier with fine tunability. Although the removable hydrogel cores were already used for the fabrication of hollow capsules as sacrificial templates, the reducible HA microgel beads used in this study are more biocompatible materials for drug delivery applications and completely dissolved out using reducing agents, compared to the previously reported hydrogel core materials.

At physiological pH, the oppositely charged two polymers (HA and PLL) are known to form a LBL multilayer film as reported earlier.^{32–34} It was reported that serial deposition of HA/PLL allowed an exponential layer growth in an early stage, followed by a linear growth phase after a certain number of depositions. In this study, serial deposition of HA/PLL

polyelectrolyte layers on the HA microgels was obtained and evaluated by measuring the ζ -potential values after each adsorption cycle (Figure 2A). Surface ζ -potential value of anionic HA microgels was $-7.8 \pm 2.6 \text{ mV}$ at pH 6.5 ($n = 5$). The ζ -potential value increased to $36.8 \pm 3.1 \text{ mV}$ after one cycle of PLL adsorption but decreased to $-18.2 \pm 5.4 \text{ mV}$, a more negative value than the bare HA microgels, after depositing HA onto the PLL adsorbed HA microgels. Alternative assembly of oppositely charged polymers onto the HA microgels exhibited a cyclic change in ζ -potential values after each adsorption, revealing that HA and PLL were successively adsorbed to form an LBL multilayer shell onto the surface of HA microgels. After constructing 10 HA/PLL bilayers on the surface, inner HA microgel cores were removed via reductive cleavages of the disulfide linkages by treatment of DTT at neutral pH. The core removal process was preformed before the shell cross-linking to avoid any undesirable cross-linking reactions between the HA core templates and HA/PLL multilayers. Hollow HA/PLL microcapsules were then collected by centrifugation and dispersed in 5 % (w/v) EDC solution for 6 h to cross-link the capsule walls by generating stable amide bonds between primary amine groups of PLL and carboxylic groups of HA.^{17,18,28}

The preparation of hollow-shell cross-linked microcapsules has been visualized under a confocal microscope (Figure 2B–D). In panels B and C of Figure 2, HA microgels conjugated with rhodamine dye and those coated with an FITC-labeled PLL/HA LBL shell layer are presented, respectively. It can be seen that LBL multilayer-coated HA microgels have a green corona layer (about $2 \mu\text{m}$) surrounding a red HA microgel inner core. A rather thick shell layer observed can be attributed to the exponential growth of HA/PLL multilayer mainly caused by dynamic diffusion process of adsorbed polyelectrolytes in the early LBL cycles, along with penetration of the polyelectrolyte layers in the HA microgel core and sticking of HA remnants to the capsules wall during the core dissolution process.^{30,32} After DTT treatment, only a green shell layer can be seen, confirming the complete removal of the HA core materials (Figure 2D). The slightly enlarged size of the hollow capsules after the hydrogel core removal might be caused by increased osmotic pressure within the inner void spaces that were filled with many ionic species.³⁵ From the confocal images, it can be concluded that the disulfide linkages between HA chains are readily cleaved in the reductive mild condition. It should be noted that the molecular weight of HA was an important factor for the production of removable HA core microgels, since high molecular weight HA could not be easily leached out through the LBL multilayer shell. When thiolated HA with high molecular weight ($1.79 \times 10^7 \text{ Da}$) was used to fabricate the core materials, HA could not be removed after the DTT treatment (data not shown). The result suggests that the molecular weight of HA as a template material must be taken into account when considering the fabricating hollow microcapsules.

Stability and pH-Responsive Permeability of Cross-Linked Hollow Microcapsules. The freeze/thaw and pH stability of shell cross-linked LBL microcapsules were examined by CLSM (Figure 3). After three consecutive cycles of freezing and thawing, structural integrities of HA/PLL microcapsules with/without cross-linking were comparatively observed under a confocal microscope (Figure 3A). In the case of un-cross-linked microcapsules, a repeated freezing and thawing process completely disrupted the microcapsule walls with the production of aggregated debris. On the other hand, cross-linked microcapsules

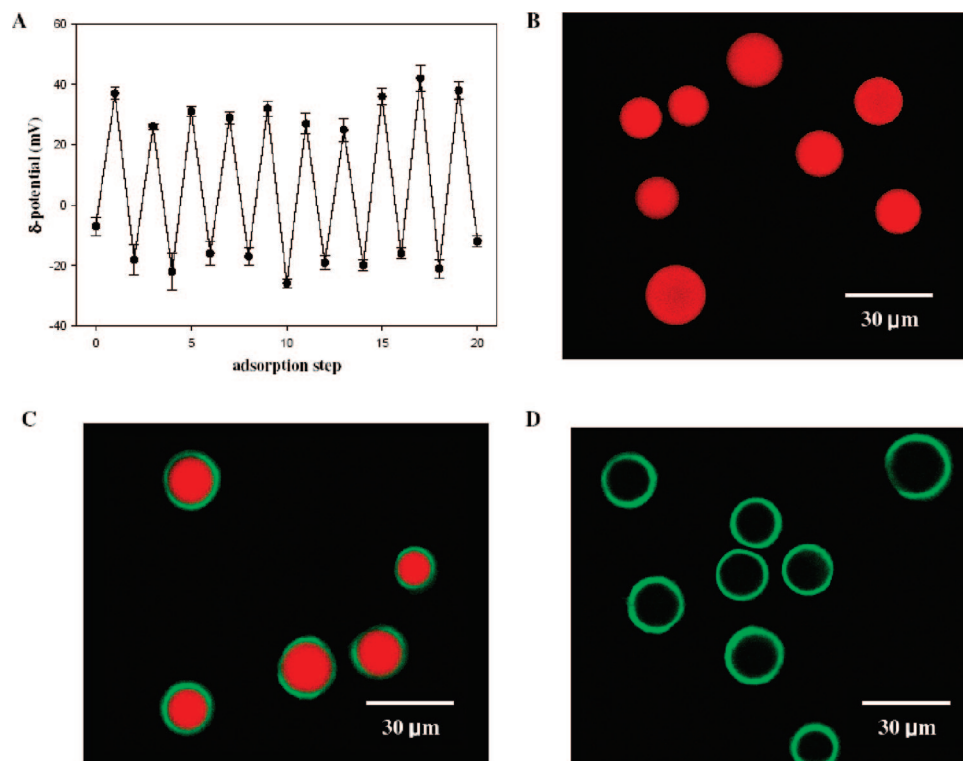


Figure 2. (A) ζ -Potential as a function of layer number during the LBL multilayer formation onto the surface of HA microgels. All measurements were carried out in deionized water at pH 6.5 ($n = 5$). Confocal laser scanning microscopy (CLSM) images of (B) rhodamine conjugated HA microgels, (C) FITC-labeled HA/PLL shell LBL multilayer encasing rhodamine conjugated HA microgels, and (D) FITC-labeled HA/PLL microcapsules after removing the HA microgel cores.

capsules maintained their hollow structures after three cycles of freezing/thawing, showing far enhanced stability against the freezing/thawing stress. It is conceivable that during the freezing process, water-filled hollow interiors encased by the weakly charge-interacted LBL walls burst out by the volume expansion induced by the formation of ice crystals. In contrast, the cross-linked microcapsules seemed to have sufficient elastic strength to withstand the volume expansion, resulting in intact hollow morphological characteristics despite repeated freezing/thawing cycles. The structural stability of microcapsules with and without shell cross-linking was also examined under very acidic condition as shown in Figure 4B. The hollow microcapsules were exposed to pH 2.0, and their structural stabilities were visualized as a function of time. The confocal images show that un-cross-linked microcapsules disappear completely within 150 s due to the disintegration of capsule wall and expansion of capsule lumen, while cross-linked microcapsules still maintain hollow structures up to 900 s. The structural stability of the hollow LBL microcapsules tolerable at cyclic freezing/thawing and acidic conditions is a very critical factor when considering their applications as drug delivery carriers. To this end, shell cross-linked HA/PLL microcapsules with hollow interiors might have good opportunities for encapsulating a wide range of drug molecules under severe formulation conditions.

The permeability of cross-linked HA/PLL microcapsules at different pH values was evaluated by CLSM using FITC-dextran (150 kDa) as a fluorescent marker. Blank microcapsule suspension in water was incubated in the FITC-dextran solution at pH 5.0 and 7.0, and their confocal images after 30 min equilibrium were taken as shown in Figure 4. It can be seen that FITC-BSA is fully permeable to the LBL wall and filled in the hollow interior at pH 5.0, whereas it cannot readily

permeate through the wall at pH 7.0. The result reveals the difference in permeability of the capsule wall at different pH values. This is due to the fact that the extent of ionic interactions between carboxylic acid groups of HA (pK_a 2.9) and primary ϵ -amine groups of PLL (pK_a 9) is highly dependent on the pH value of incubation medium. The degree of charge interactions in the cross-linked LBL shell was more reduced at pH 5.0 than at pH 7.0, resulting in a more swollen and permeable microcapsule wall structure. This finding is consistent with the previous results reporting similar pH-dependent permeability change for LBL polyelectrolyte networks.^{7,9,16,36}

pH-Dependent and Enzyme-Mediated Sustained Release of FITC-BSA from Cross-Linked Hollow Microcapsules. After FITC-BSA was loaded within the cross-linked hollow microcapsules at pH 5.0, release profiles of FITC-BSA were evaluated at pH 5.0 and 7.0 using a fluorophotometer (Figure 5). The confocal images of microcapsules encapsulating FITC-BSA are also shown in Figure 5 inset. As expected from the pH-responsive permeation results, FITC-BSA was released out faster at pH 5.0 than at pH 7.0. It is likely that the more swollen and permeable structure of capsule walls at lower pH allowed rapid release of encapsulated FITC-BSA from the microcapsules. At neutral pH, a sustained release pattern of FITC-BSA without an initial burst was observed over 5 h. The sustained release behavior of FITC-BSA might be dependent on the molecular weight of encapsulated macromolecules as well as the microstructure of cross-linked polyelectrolyte multilayer.^{8,36} In addition to pH-dependent sustained release, enzyme-mediated release of FITC-BSA from the microcapsules was investigated. Enzymatic degradation of the capsule wall is particularly interesting since the wall properties of the drug carrier can be readily changed upon varying enzyme concentrations.^{37,38} HA is a natural polymer which can be readily degraded by

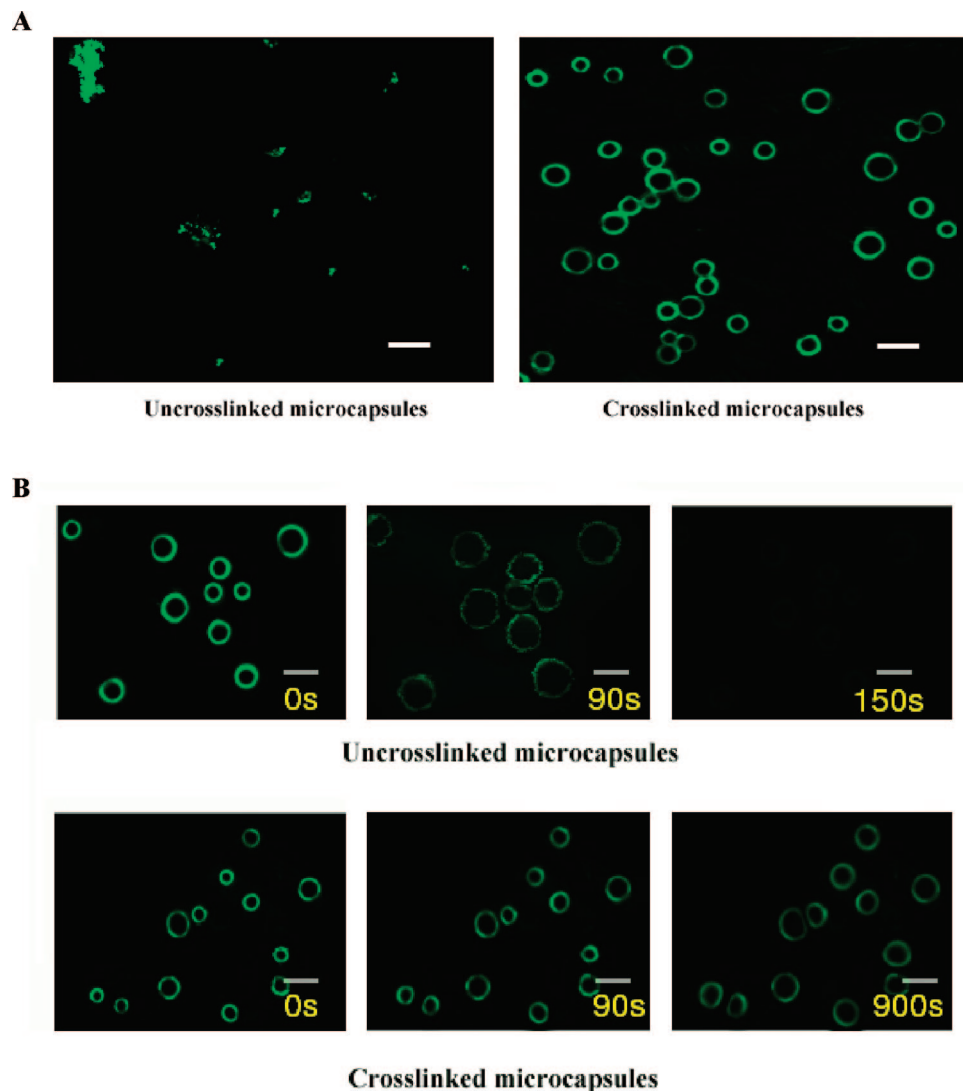


Figure 3. CLSM images of hollow microcapsules treated with various external stresses: (A) freeze/thawing and (B) pH alteration to pH 2.0. Note that the effect of EDC cross-linking was compared to un-cross-linked microcapsules. Scale bar = 20 μm .

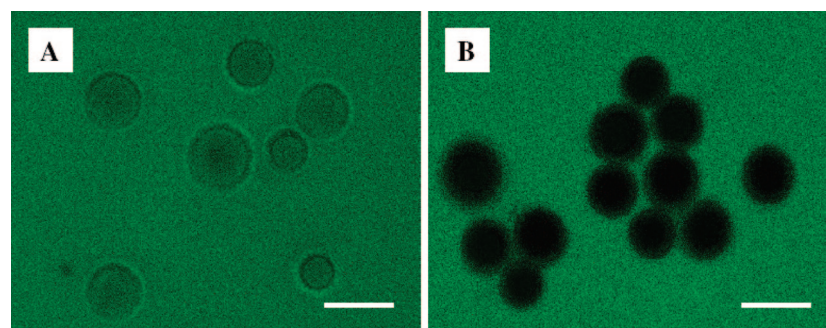


Figure 4. CLSM images of hollow microcapsules incubated with FITC-dextran (150k Da) at (A) pH 5.0 and (B) pH 7.0. Scale bar = 20 μm .

hyaluronidase. Since the structural integrity of a HA/PLL multilayer shell is crucial to the permeability, an exposure of the microcapsules to hyaluronidase was expected to facilitate the release of FITC-BSA by increasing the capsule permeability due to the cleavage of HA chains. As shown in Figure 5B, the HA/PLL microcapsules, upon the addition of 50 units/mL hyaluronidase in the buffer solution, exhibited more accelerated release of FITC-BSA than those treated with 10 units/mL hyaluronidase, suggesting that the FITC-BSA release profiles

could be readily modulated by the amount of enzyme in the incubating medium.

Cytotoxicity of Cross-Linked Hollow Microcapsules. Cross-linked HA/PLL microcapsules should demonstrate low cytotoxicity for clinical applications. NIH3T3 and C2C12 cells were cultivated in the presence of microcapsules to test cell cytotoxicity. As shown in Figure 6, there was no apparent cytotoxic effect of cross-linked HA/PLL microcapsules up to a concentration of 1 mg/mL (cell viability up to 90%). The result is

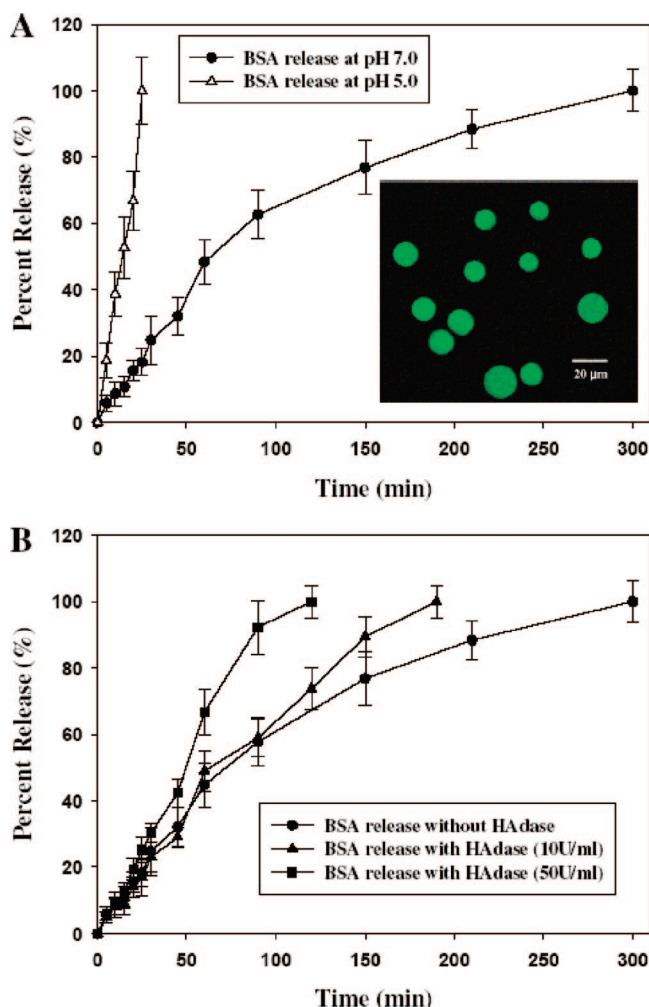


Figure 5. Cumulative percent release of FITC-BSA (66 kDa) from cross-linked microcapsules ($n = 10$) at different conditions. (A) FITC-BSA release was measured at pH 5.0 and pH 7.0. Note that the inset shows the CLSM image of FITC-BSA encapsulating microcapsules. (B) FITC-BSA release was measured at pH 7.0 with different amounts of hyaluronidase (10 and 50 units/mL).

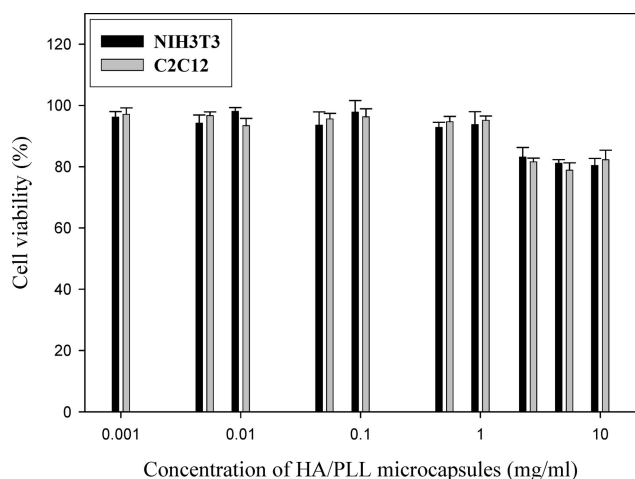


Figure 6. Cytotoxicity of cross-linked HA/PLL microcapsules using NIH3T3 and C2C12 cells.

accordance with a previous study of culturing cells on cross-linked HA/PLL polyelectrolyte multilayer films.³⁴ Thus, the cross-linked HA/PLL microcapsules can be safely used for delivering bioactive macromolecular drugs as biocompatible reservoir-type carriers.

Conclusions

Novel shell cross-linked LBL polyelectrolyte microcapsules could be prepared by alternative adsorption of HA and PLL onto the surface of HA core microgels cross-linked with disulfide linkages, removal of core HA microgels by reductive digestion, and covalent cross-linking of the remnant HA/PLL shell LBL layer. The cross-linked hollow HA/PLL microcapsules showed far enhanced stability under harsh formulation conditions while maintaining a pH responsive permeability change. With the pH-responsive permeability of the microcapsule wall, FITC-BSA was encapsulated within the HA/PLL microcapsules at acidic pH and could be released out in a controlled manner at neutral pH. The enzyme-sensitive capsule wall exhibited accelerated release of encapsulated protein drugs in the presence of hyaluronidase. The cross-linked HA/PLL microcapsules could be utilized as noncytotoxic carriers for various macromolecular drugs.

Acknowledgment. This study was supported by a National Research Laboratory grant from the Ministry of Science and Technology, Republic of Korea.

References and Notes

- (1) Shi, X.; Shen, M.; Moehwald, H. *Prog. Polym. Sci.* **2004**, *29*, 987–1019.
- (2) Donath, E.; Sukhoroukov, G. B.; Garuso, F.; Davis, S.; Moehwald, H. *Angew. Chem., Int. Ed.* **1998**, *37*, 2202–2205.
- (3) Qiu, X.; Leporatti, S.; Donath, E.; Moehwald, H. *Langmuir* **2001**, *17*, 5375–5380.
- (4) Caruso, F.; Caruso, R. A.; Moehwald, H. *Science* **1998**, *282*, 1111–1114.
- (5) Antipov, A. A.; Shchukin, D. G.; Fedutik, Y.; Zhanavskina, I.; Klechkovskaya, V.; Sukhoroukov, G. B.; Moehwald, H. *Macromol. Rapid Commun.* **2003**, *24*, 274–277.
- (6) Shchukin, D. G.; Radtchenko, I. L.; Sukhoroukov, G. B. *Mater. Lett.* **2003**, *57*, 1743–1747.
- (7) Sukhoroukov, G. B.; Antipov, A. A.; Voigt, A.; Donath, E.; Moehwald, H. *Macromol. Rapid Commun.* **2001**, *22*, 44–46.
- (8) Ibarz, G.; Daehne, L.; Donath, E.; Moehwald, H. *Macromol. Rapid Commun.* **2002**, *23*, 474–478.
- (9) Dejgnet, C.; Sukhoroukov, G. B. *Langmuir* **2004**, *20*, 7265–7269.
- (10) De Geest, B. G.; Sanders, N. N.; Sukhoroukov, G. B.; Demeester, J.; De Smedt, S. C. *Chem. Soc. Rev.* **2007**, *36*, 636–649.
- (11) Sukhoroukov, G. B.; Rogach, A. L.; Garstka, M.; Springer, S.; Parak, W. J.; Munoz-Javier, A.; Kreft, O.; Skirtach, A. G.; Susha, A. S.; Ramaye, Y.; Palankar, R.; Winterhalter, M. *Small* **2007**, *3*, 944–955.
- (12) Ibarz, G.; Daehne, L.; Donath, E.; Moehwald, H. *Adv. Mater.* **2001**, *13*, 1324–1327.
- (13) Radt, B.; Caruso, F. *Adv. Mater.* **2004**, *16*, 2184–2189.
- (14) De Geest, B. G.; Jonas, A. M.; Demeester, J.; De Smedt, S. C. *Langmuir* **2006**, *22*, 5070–5074.
- (15) An, Z.; Moehwald, H.; Li, J. *Biomacromolecules* **2006**, *7*, 580–585.
- (16) Tong, W.; Gao, C.; Moehwald, H. *Macromolecules* **2006**, *39*, 335–340.
- (17) Mauser, T.; Dejgnet, C.; Sukhoroukov, G. B. *Macromol. Rapid Commun.* **2004**, *25*, 1781–1785.
- (18) Schuetz, P.; Caruso, F. *Adv. Funct. Mater.* **2003**, *13*, 929–937.
- (19) Pastoriza-Santos, I.; Scholer, B.; Caruso, F. *Adv. Funct. Mater.* **2001**, *11*, 122–128.
- (20) Zhao, Q.; Mao, Z.; Gao, C.; Shen, J. *J. Biomater. Sci., Polym. Ed.* **2006**, *17*, 997–1014.
- (21) Garza, J. M.; Lavalle, P. *Langmuir* **2005**, *21*, 12372–12377.
- (22) Shenoy, D. B.; Sukhoroukov, G. B. *Macromol. Biosci.* **2005**, *5*, 451–458.
- (23) Larsen, N. E.; Balazs, E. A. *Adv. Drug Delivery Rev.* **1991**, *7*, 279–293.
- (24) Lee, H.; Mok, H.; Lee, S.; Oh, Y.; Park, T. G. *J. Controlled Release* **2007**, *119*, 245–252.
- (25) Kim, M.; Park, T. G. *J. Controlled Release* **2002**, *80*, 69–77.
- (26) Arvinte, T.; Cudd, A.; Drake, A. F. *J. Biol. Chem.* **1993**, *268*, 6415–6422.

- (27) Gao, C. Y.; Mohwald, H.; Shen, J. C. *Adv. Mater.* **2003**, *15*, 930–933.
- (28) Mauser, T.; Dejugnat, C.; Moehwald, H.; Sukhorukov, G. B. *Langmuir* **2006**, *22*, 5888–5893.
- (29) Bae, K.; Park, T. G. *Biomacromolecules* **2007**, *8*, 650–656.
- (30) De Geest, B. G.; Dejugnat, C.; Prevot, M.; Sukhorukov, G. B.; Demeester, J.; De Smedt, S. C. *Adv. Funct. Mater.* **2007**, *17*, 531–537.
- (31) Zhu, H.; McShane, M. *Bioconjugate Chem.* **2005**, *16*, 1451–1458.
- (32) Picart, C.; Mutterer, J.; Richert, L.; Luo, Y.; Prestwich, G. D.; Schaaf, P.; Voegel, J. C.; Lavalle, P. *Proc. Natl. Acad. Sci. U.S.A.* **2002**, *99*, 1252–1255.
- (33) Porcel, C.; Lavalle, P.; Ball, V.; Decher, G.; Senger, B.; Voegel, J. C.; Schaaf, P. *Langmuir* **2006**, *22*, 4376–4383.
- (34) Schneider, A.; Picart, C.; Senger, B.; Schaaf, P.; Voegel, J. C.; Frisch, B. *Langmuir* **2007**, *23*, 2655–2662.
- (35) Gao, C. Y.; Moya, S.; Lichtenfeld, H.; Casoli, A.; Fiedler, H.; Donath, E.; Mohwald, H. *Macromol. Mater. Eng.* **2001**, *286*, 355–361.
- (36) Antipov, A. A.; Sukhorukov, G. B.; Leporatti, S.; Radtchenko, I. L.; Donath, E.; Mohwald, H. *Colloids Surf.* **2002**, *198*, 535–541.
- (37) De Geest, B. G.; Vandenbroucke, R. E.; Guenther, A. M.; Sukhorukov, G. B.; Hennink, W. E.; Sanders, N. N.; Demeester, J.; De Smedt, S. C. *Adv. Mater.* **2006**, *18*, 1005–1009.
- (38) Itoh, Y.; Matsusaki, M.; Kida, T.; Akashi, M. *Biomacromolecules* **2007**, *7*, 2715–2718.

BM700854J